DOI: 10.1002/chem.200800244

Mono- and Diprotonation of the Superbasic Bisguanidine 1,2-Bis(*N*,*N*,*N*′,*N*′-tetramethylguanidino)benzene (btmgb) and Pt^{II} and Pt^{IV} Complexes of Chelating Bisguanidines and Guanidinates

Anastasia Peters, Ute Wild, Olaf Hübner, Elisabeth Kaifer, and Hans-Jörg Himmel*[a]

Abstract: New Pt complexes of chelating bisguanidines and guanidinate ligands were synthesized and characterized. 1,2-Bis(*N*,*N*,*N*′,*N*′-tetramethylguanidino)benzene (btmgb) was used as a neutral chelating bisguanidine ligand, and 1,3,4,6,7,8-hexahydro-2*H*-pyrimido-[1,2-*a*]pyrimidinate (hpp^-) as a guanidinate ligand. The salts $[btmgbH]^+[HOB(C_6F_5)_3]^-$ and $[btmgbH_2]Cl_2$ and the complexes $[(btmgb)PtCl_2]$, $[(btmgb)PtCl(dmso)]^+[PtCl_3(dmso)]^-$, and $[(btmgb)PtCl(dmso)]^+[Cl^-]$ were synthesized and characterized. In the $[btmgbH]^+$ cation the proton is bound to only one N atom. In the other complexes, both imine N atoms are coordinated to the Pt^{II}, thus adopting a η^2-coordinational mode. The hpp^- anion, which usually prefers a bridging binding mode in dinuclear complexes, is η^2-coordinated in the Pt^{IV} complex $[(\eta^2\text{-hpp})(hppH)PtCl_2\{N(H)C(O)CH_3\}]$, which is formed (in low yield) by reaction between *cis*-$[(hppH)_2PtCl_2]$ and H_2O_2 in CH_3CN.

Keywords: chelates · guanidinates · guanidines · platinum · structure elucidation

Introduction

Interest in guanidine and its derivatives is manifold: for example, it has been shown that 1,2-bis(*N*,*N*,*N*′,*N*′-tetramethylguanidino)naphthalene (btmgn)[1] is a superbasic and kinetically active proton sponge. Guanidinium chloride is, like urea, a denaturant, which destabilizes globular proteins.[2] The destabilization mechanism is as yet unclear despite intensive research on protonated guanidines.[3] The potential use of guanidine derivatives as synthetic anion receptors (for example, in complexation of carboxylates and diols) has been studied in some detail.[4,5] The application of these molecules as ligands in molecular complexes of transition metals, however, is still very underdeveloped. Bridged bisguanidine molecules which have been synthesized[6] include 1,2-bis(*N*,*N*,*N*′,*N*′-tetramethylguanidino)ethane[7] (btmge), 1,3-bis(*N*,*N*,*N*′,*N*′-tetramethylguanidino)propane[8] (btmgp), 1,2-bis(*N*,*N*,*N*′,*N*′-tetramethylguanidino)benzene[9] (btmgb), 1,8-bis(*N*,*N*,*N*′,*N*′-tetramethylguanidino)naphthalene[1] (btmgn), and 2,2′-bis(*N*,*N*,*N*′,*N*′-tetramethylguanidino)biphenyl (btmgbp)[10]. Rare examples of structurally characterized

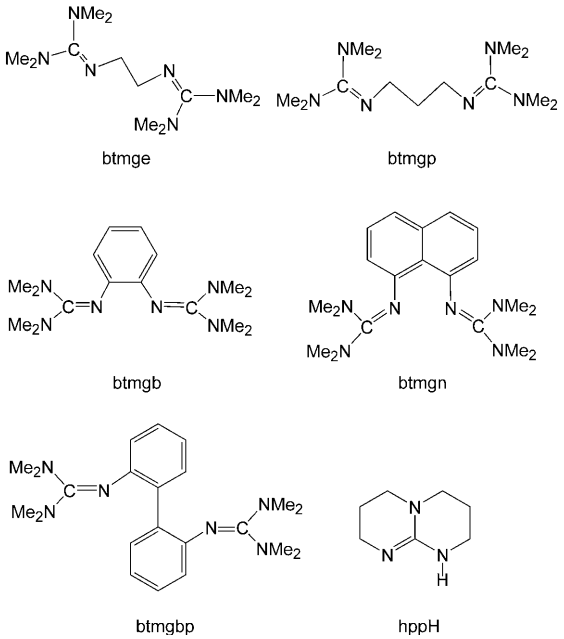

[a] A. Peters, U. Wild, Dr. O. Hübner, Dr. E. Kaifer, Prof. Dr. Dr. H.-J. Himmel
Anorganisch-Chemisches Institut
Ruprecht-Karls-Universität Heidelberg
Im Neuenheimer Feld 270, 69120 Heidelberg (Germany)
Fax: (+49) 6221-54-5707
E-mail: hans-jorg.himmel@aci.uni-heidelberg.de

Supporting Information for this article (IR, NMR, and UV/Vis spectra, isodensity surfaces, and calculated results for the btmgb ligand and its complexes) is available on the WWW under http://dx.doi.org/10.1002/chem.200800244 or from the author.

transition metal complexes include the CuI, $CuCl_2$, and FeI_2 complexes of btmgp.[8] Owing to their strong basicity, complexes with guanidine ligands should have interesting properties. Hence with the tripodal tren (tris(2-aminoethyl)amine) derivative tris(tetramethylguanidino)tren ($(tmg)_3$tren), the cationic Cu complex $[(tmg)_3trenCu]^+$[11] has been synthesized and was shown recently to bind O_2 in an end-on fashion.[12] Very recently it has been shown that this Cu^{II} superoxo complex can be used in oxygenation reactions.[13] Another example is $[Pd(tmg)_4]Cl_2$, which has been introduced as an inexpensive, air-stable catalyst for Heck reactions.[14]Herein we report on the synthesis of Pt^{II} and Pt^{IV}

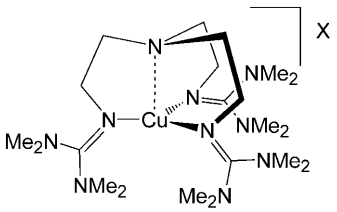

$[(TMG)_3trenCu]X$ (X = Cl or ClO_4)

complexes with the chelating ligands bisguanidine (btmgb) and the guanidinate derivative (1,3,4,6,7,8-hexahydro-2*H*-pyrimido[1,2-*a*]pyrimidinate) (hpp^-). We also report on the first structural characterization of the $[btmgbH]^+$ cation and the $[btmgbH_2]^{2+}$ dication.

Results and Discussion

We report on the characterization of the neutral and mono- and diprotonated btmgb ligand, the synthesis of Pt^{II} complexes of the btmgb ligand and their structural and electronic properties, and the synthesis of a Pt^{IV} complex with the η^2-coordinating guanidinate derivative hpp^- occupying two coordination sites in a distorted octahedral complex.

Neutral and protonated btmgb ligands: We first studied the reaction between btmgb and $B(C_6F_5)_3$. As expected, a complex $[(btmgb)\cdot B(C_6F_5)_3]$ cannot be formed for steric reasons. In contrast to the reaction between 1,8-bis(dimethylamino)-naphthalene and $B(C_6F_5)_3$ [see Eq. (1)],[15] $B(C_6F_5)_3$ seems not to abstract an H^- from btmgb. Thus btmgb/$B(C_6F_5)_3$ represents a "frustrated" Lewis acid–base pair.

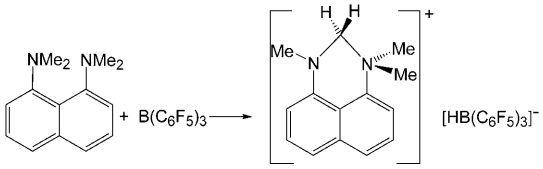

Unfortunately, this mixture shows no reaction with H_2 (1 bar, 25 °C), so most probably it cannot be used like the recently developed moisture and air-stable phosphonium borates $[R_2PH(C_6F_4)BH(C_6F_5)_2]$ (R = 2,4,6-$Me_3C_6H_2$ or *t*Bu) for hydrogenation reactions.[16] However, btmgb reacts with $H_2O\cdot B(C_6F_5)_3$ to give the salt $[btmgbH]^+[HOB(C_6F_5)_3]^-$, **1**. Crystals of **1** suitable for X-ray diffraction analysis were grown from CH_3CN. This complex is the first salt of the protonated ligand to be structurally characterized. The addition of H^+ can be regarded as the simplest model for complexes of btmgb. Two details of the structure of **1** (see Figure 1) are

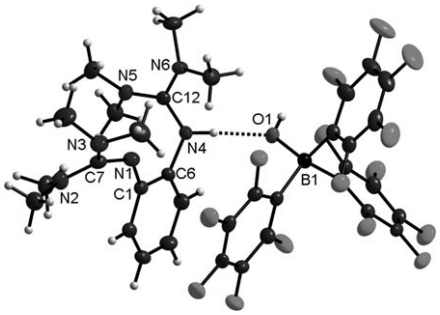

Figure 1. Crystal structure of **1**. Ellipsoids are drawn at the 50% probability level.

of particular interest: a) in clear contrast to protonated proton sponges such as 1,8-bis(dimethylamino)naphthalene or 1,8-bis(*N*,*N*,*N*′,*N*′-tetramethylguanidino)naphthalene, H^+ is bound to only one of the imine N atoms in btmgb, and in addition interacts with the O atom of the $[HOB(C_6F_5)_3]^-$ anion; b) as a consequence of protonation, the N=C bond length increases by approximately 4 pm (from 130.1(3) to 134.0(3) pm, see Table 2). Table 1 contains selected bond lengths and angles of **1**. The cation and anion interact through an N–H···O contact. The structure of the $[HOB(C_6F_5)_3]^-$ anion is close to that found previously in the salt of the 7-aza-1*H*-indolium cation.[17]

Table 1. Selected bond lengths [pm] and angles [°] of **1** as obtained by X-ray diffraction studies (see Figure 1 for atom numbering).

N1–C1	139.7(3)	N4–C6	143.4(3)
N1–C7	129.7(3)	N4–C12	134.0(3)
C7–N2	137.3(3)	C12–N5	134.6(3)
C7–N3	137.5(3)	C12–N6	133.9(3)
N4–H	89.3(2)	O1–H	89.0(2)
N4···O1	277.3(2)	O1–B1	146.6(3)
N1···N4	276.8(3)	C1–C6	140.9(3)
N4–H···O	176.7(54)	NH···O1–B1	138.3(54)
N4-H···N3	42.7(54)	H-O-B1	116.3(46)
C6-N4-C12	124.18(17)	C1-N1-C7	123.49(18)
N4-C12-N5	120.38(19)	N1-C7-N2	127.97(19)
N4-C12-N6	119.50(18)	N1-C7-N3	118.06(19)
N5-C12-N6	120.02(19)	N2-C7-N3	113.96(18)

The free $[btmgbH]^+$ cation has been studied previously by using quantum chemical calculations,[18] which found an N–H bond length of 99.7 pm in the minimum-energy struc-

ture. The distance between of the proton from the second imine N atom amounts to 255.9 pm. Thus, in agreement with the results obtained for **1**, the calculations predict that the proton will be bound to only one N atom and will not interact significantly with the second one. We recalculated the structures of the neutral btmgb molecule and the $[btmgbH]^+$ cation; Table 2 compares some of the structural

Table 2. Comparison of calculated and experimentally determined bond lengths [pm] and angles [°], and degree of pyramidalization of amino nitrogen [%] for btmgb and $[btmgbH]^+$ (see Figures 1 and Scheme 1, and the Supporting Information, for atom numbering and nomenclature).[a]

	btmgb		$[btmgbH]^+$	
	exptl[b]	calcd	exptl	calcd
C1–C6	141.8(3)	141.7(4)	140.9(3)	141.4(6)
N1···N4	285.8(2)	288.1(0)	276.8(3)	280.2(9)
C1–N1/(C–N)$_{ip}$	141.0(3)	140.7(0)	139.7(3)	138.2(4)
C2–N4/(C–N)$_{dp}$	140.4(3)	139.5(7)	143.4(3)	143.7(5)
N1–C7/(C–N)$_{ip}$	129.1(3)	128.5(5)	129.7(3)	131.0(8)
N4–C12/(C–N)$_{dp}$	130.1(3)	128.8(8)	134.0(3)	134.4(0)
C7–N2/(C–N)$_{ip1}$	138.1(3)	138.5(7)	137.3(3)	137.7(7)
C7–N3/(C–N)$_{ip2}$	138.8(3)	139.5(1)	137.5(3)	136.8(6)
C12–N5/(C–N)$_{dp1}$	138.5(3)	139.0(6)	134.6(3)	134.6(2)
C12–N6/(C–N)$_{dp2}$	137.6(3)	138.9(4)	133.6(3)	134.3(1)
N–H			89.3(2)	100.9(4)
H···N			335.7(3)	340.9(0)
β			42.70(9)	45.96
DP(N$_{dp1}$)	2.1	2.1	0.3	0.8
DP(N$_{dp2}$)	9.7	8.5	8.1	4.3
DP(N$_{ip1}$)	10.6	11.0	0.3	0.2
DP(N$_{ip2}$)	3.8	3.1	1.1	0.6

[a] N2 apical: DP(N$_{ip1}$); N3 apical: DP(N$_{ip2}$); N5 apical: DP(N$_{dp1}$); N6 apical: DP(N$_{dp2}$) (DP = degree of pyramidalization; dp,ip = directly and indirectly protonated). [b] Parameters from a new X-ray diffraction analysis (see cif file, CCDC-677131).

elements. The nomenclature (which is similar to that used in ref. [18]) is explained in Scheme 1 (DP: degree of pyramidalization).[18,19] In agreement with the previous calculations

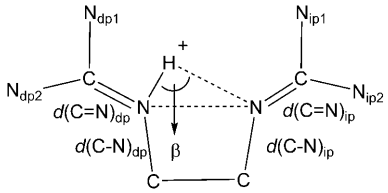

Scheme 1. Labeling for the $[btmgbH]^+$ cation.

and our experimental results obtained for **1**, the form in which the proton is bound to only one N atom represents a minimum on the potential energy surface.[20] The change in the calculated N···N separation from 288.1 pm in btmgb to 280.2 pm in $[btmgbH]^+$ is particularly remarkable. The value of 218.4 pm as given in ref. [18]) for the N···N separation in noncoordinating btmgb is a printing error; it should be 281.4 pm.[45] The crystal structure analysis yielded N···N separations of 285.8(2) and 276.8(3) pm in btmgb and **1**.

A $[btmgbH_2]^{2+}$ dication is present in the salt $[btmgbH_2]Cl_2$, **2**, which can be synthesized from btmgb and HCl and crystallized from CH_3CN (and contains crystal water). Figure 2 displays the crystal structure and Table 3 summarizes some of the structural parameters. The elongation of the N1–C7 and N4–C12 bond lengths from 129.1(3)/130.1(3) pm in btmgb to 135.1(3)/135.8(3) pm in **2** is the most remarkable feature and was found also for the Pt complexes studied in this work (see below). Only one of the two Cl^- anions interacts with the H atoms of the two NH groups. The distance between the two Cl^- anions amounts to more than 650 pm to minimize the electrostatic repulsion.

Pt complexes of btmgb: If the btmgb ligand is reacted with $[(dmso)_2PtCl_2]$, different products are obtained depending on the solvent. As a reaction product in CH_3CN we obtained a red salt, which was identified as $[(btmgb)PtCl(dmso)]^+$ $[PtCl_3(dmso)]^-$, **3** (see Scheme 2). Crystals of **3** were grown from acetone/hexane. Figure 3 illustrates the crystal structure of **3** and Table 4 con-

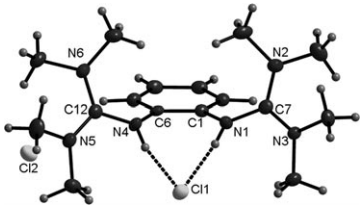

Figure 2. Crystal structure of **2**. Ellipsoids are drawn at the 50% probability level.

tains selected bond lengths and angles. In contrast to H^+, Pt^{II} is bound to both imine N atoms (N1 and N4). The Pt–Cl length (231.7(1) pm) in the cation $[(btmgb)PtCl(dmso)]^+$ is slightly greater than that measured for (2,2′-bipyridine)dichloroplatinum (230.6 pm),[21] and significantly greater than the Pt–Cl bond length measured in the unusual complex dichloro[4,9-dichloroquino(7,8*h*)quinoline]platinum (229.2(4) pm), in which the Pt atom lies above the approximate plane in which the quinoline ligand (which becomes bent upon coordination) is located.[22] The relatively great Pt–Cl bond length in **3** can be explained by the electron density donation by the strongly basic btmgb ligand. The Pt–N bond lengths, 203.6(3) and 201.5(3) pm, are in good

Table 3. Selected bond lengths [pm] and angles [°] of **2** as obtained by X-ray diffraction studies (see Figure 2 for atom numbering).

C1–N1	145.8(4)	C6–N4	142.8(3)
N1–C7	135.1(3)	N4–C12	135.8(3)
C7–N2	132.2(4)	C12–N6	133.1(3)
C7–N3	133.8(3)	C12–N5	133.5(3)
Cl1···HN1	225.8(2)	Cl1···HN4	230.4(2)
N1–H	89(3)	N4–H	90(3)
C1–C6	139.6(4)	N1···N4	283.9(3)
C7-N1-H	117(2)	C12-N4-H	116.4(19)
C1-N1-H	115(2)	C6-N4-H	118.9(19)
C1-N1-C7	125.5(2)	C6-N4-C12	123.8(2)
N1-C7-N2	118.8(2)	N4-C12-N6	120.9(2)
N1-C7-N3	120.4(3)	N4-C12-N5	118.0(2)
N2-C7-N3	120.7(2)	N5-C12-N6	121.1(2)

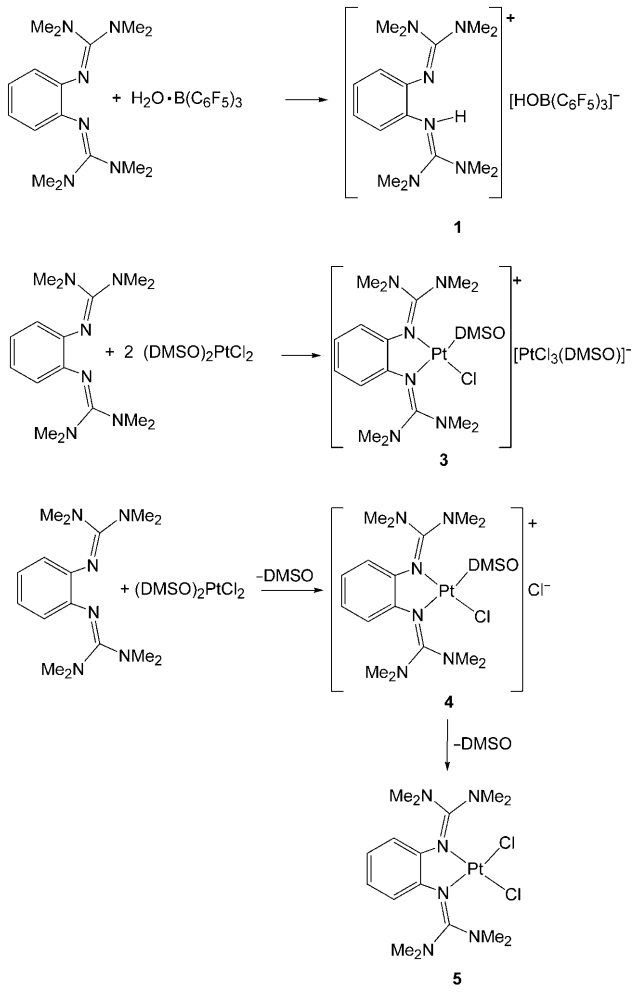

Scheme 2. Synthesis of complexes **1**,**3**–**5**.

agreement with those obtained previously for the guanidine complex $[(hppH)_2PtCl_2]$ in its *cis* (202.3(3) and 202.2(3) pm) and *trans* (203.3(2) pm) forms.[23] They compare with a Pt–N bond length of 200.1(6) pm in (2,2′-bipyridine)dichloroplatinum.[20] The Pt atom is coordinated in a planar fashion (angle sum = 360°) by the four atoms (Cl, S, and two N) directly attached to Pt. Whereas all these parameters fit more or less with expectations, the dramatic change in the btmgb C=N bond lengths within the btmgb ligand upon coordination is remarkable. Thus the N1–C7 and N4–C12 bond lengths increase from 129.1 and 130.1 pm in btmgb to as much as 135.6(5) and 137.5(5) pm in **3**.

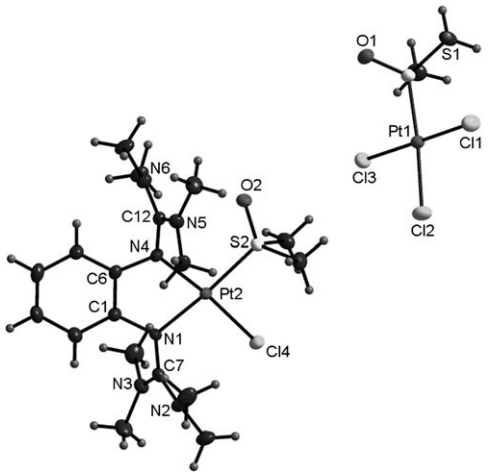

Figure 3. Crystal structure of **3**. Ellipsoids are drawn at the 50% probability level.

Table 4. Selected bond lengths [pm] and angles [°] of **3** as obtained by X-ray diffraction studies (see Figure 3 for atom numbering).

N1–C1	141.1(5)	N4–C6	140.6(5)
N1–C7	135.6(5)	N4–C12	137.5(5)
C7–N2	133.6(5)	C12–N5	132.0(5)
C7–N3	134.3(5)	C12–N6	134.4(5)
N1–Pt2	203.6(3)	N4–Pt2	201.5(3)
Pt2–Cl4	231.7(1)	Pt2–S2	221.3(1)
Pt1–S1	219.6(1)	Pt1–Cl1	230.4(1)
Pt1–Cl2	232.8(1)	Pt1–Cl3	230.5(1)
S1–O1	147.4(3)	S2–O2	147.1(3)
N1-Pt2-N4	79.96(13)	Cl4-Pt2-S2	88.87(4)
N1-Pt2-Cl4	94.05(9)	N4-Pt2-S2	96.99(10)
N1-Pt2-S2	174.07(10)	N4-Pt2-Cl4	173.86(9)
C6-N4-Pt2	114.8(2)	C1-N1-Pt2	113.8(2)
C12-N4-Pt2	126.7(2)	C7-N1-Pt2	124.9(2)
C6-N4-C12	117.5(3)	C1-N1-C7	120.2(3)
N4-C12-N5	119.1(3)	N1-C7-N2	119.6(3)
N4-C12-N6	119.2(3)	N1-C7-N3	121.3(4)
N5-C12-N6	121.6(3)	N2-C7-N3	119.1(4)

Additional experiments were carried out with btmgb and $[(dmso)_2PtCl_2]$ dissolved in DMSO. The product of this reaction (see Scheme 2) turned out to be the salt $[(btmgb)PtCl(dmso)]^+Cl^-$, **4**, which was identified by NMR, IR, UV/Vis spectroscopy, and mass spectrometry. If **4** is heated under vacuum to 150 °C, the NMR spectra indicates the loss of DMSO and quantitative formation of the neutral complex $[(btmgb)PtCl_2]$, **5**. DMSO elimination of this kind was also observed for other Pt complexes; for example, reaction between $[(dmso)_2PtCl_2]$ and ethylenediamine (en) yields first [PtCl(dmso)(en)]Cl,[24] which can be converted into $[(en)PtCl_2]$ by heating in vacuum or by stirring in CH_2Cl_2

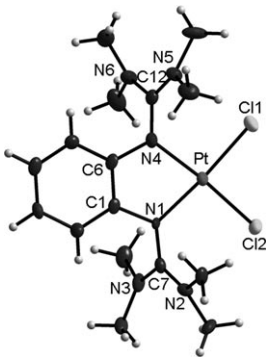

Figure 4. Crystal structure of **5**. Ellipsoids are drawn at the 50% probability level.

for several days.[25] Crystals of **5** were grown from toluene/dichloromethane (6:1 v/v) mixtures. As in **3** (and also **2**), the significant elongation of the btmgb C=N bond lengths in **5** upon coordination, as determined by X-ray diffraction (Figure 4), is the most remarkable structural detail (see Table 5 for selected bond lengths and angles). Quantum chemical calculations are generally in pleasing agreement with

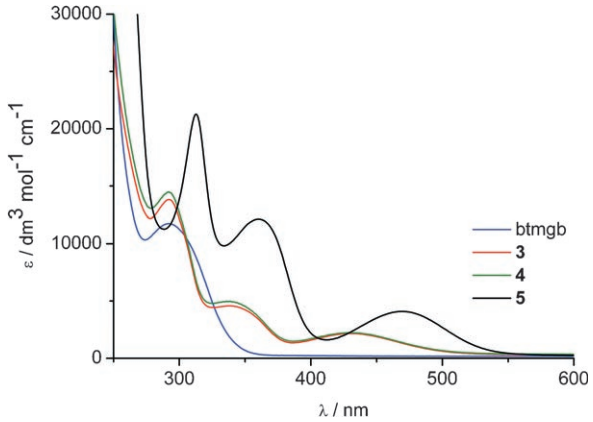

Figure 5. UV/Vis spectra of btmgb and compounds **3**–**5**.

Table 5. Selected bond lengths [pm] and angles [°] of **5** as obtained by X-ray diffraction studies (see Figure 4 for atom numbering).

N1–C7	136.0(8)	N4–C12	135.2(8)
N1–C1	141.7(7)	N4–C6	141.5(8)
C7–N2	131.2(8)	C12–N5	131.6(8)
C7–N3	134.7(8)	C12–N6	135.9(8)
N1–Pt	202.3(5)	N4–Pt	203.3(5)
Pt–Cl1	232.0(2)	Pt–Cl2	232.0(2)
N1-Pt-N4	80.6(2)	Cl1-Pt-Cl2	88.96(6)
N1-Pt-Cl1	174.64(14)	N1-Pt-Cl2	94.89(14)
N4-Pt-Cl1	95.23(15)	N4-Pt-Cl2	173.15(15)
C6-N4-Pt	113.8(4)	C1-N1-Pt	113.7(4)
C12-N4-Pt	125.0(4)	C7-N1-Pt	125.5(4)
C6-N4-C12	119.2(5)	C1-N1-C7	118.8(5)
N4-C12-N5	120.2(6)	N1-C7-N2	120.4(6)
N4-C12-N6	120.2(6)	N1-C7-N3	120.5(6)
N5-C12-N6	119.5(6)	N2-C7-N3	119.1(6)

Table 6. Measured absorptions [nm], with extinction coefficients [$dm^3 mol^{-1} cm^{-1}$] in parentheses, for btmgb and complexes **3**, **4**, and **5**.

$[(dmso)_2PtCl_2]$	btmgb	**3**	**4**	**5**
265 (3.80×10^3)	292 (1.18×10^4)	292 (1.45×10^4)	292 (1.38×10^4)	313 (2.13×10^4)
		341 (0.49×10^4)	341 (0.46×10^4)	361 (1.21×10^4)
		431 (0.22×10^4)	432 (0.22×10^4)	469 (0.41×10^4)

the experimental results (see the tables in the Supporting Information); the largest deviations occur for the N–Pt bond lengths. The N1–C7 and N4–C12 bond lengths in **5** were calculated to be 134.0 and 133.9 pm. In principle **5** can be converted back to **4** on stirring a solution of **5** in DMSO. However, this reaction is extremely slow and requires more than a week at room temperature. $[(en)PtCl_2]$ has been shown previously to undergo slow solvolysis in DMSO at room temperature to give $[(en)Pt(dmso)Cl]^+$ $[Cl]^-$;[26] this reaction can be accelerated by UV photolysis.[27] The Gibbs energy of activation for the thermal process was estimated to be 96 kJ mol^{-1} at 25 °C.

Figure 5 displays UV/Vis spectra for free btmgb and **3**–**5**, and Table 6 includes the wavelengths and extinction coefficients for all the absorption maxima observed. The wavelength of the absorption maximum of $[(dmso)_2PtCl_2]$ was taken from the literature.[28] The spectrum of the free btmgb ligand contains an absorption maximum at $\lambda = 292$ nm. In the spectra recorded for **3**, **4**, and **5**, three absorption maxima were observed. As expected, the spectra of **3** and **4** are similar. The absorption maxima shift to lower energies in the neutral complex **5**. Information about the electron density distributions in the HOMO and LUMO of free btmgb **5** and the $[(btmgb)PtCl(dmso)]^+$ cation present in **3** and **4** was obtained by quantum chemical calculations. An illustration of the isodensity surfaces (see the Supporting Information) reveals that the HOMOs of free btmgb and the $[(btmgb)PtCl(dmso)]^+$ cation have some similarities, and the Pt d orbital contribution is not very substantial. Only in the LUMO of $[(btmgb)PtCl(dmso)]^+$ is a large contribution from a Pt d orbital visible. In the HOMO of **5**, however, a Pt d orbital plays a dominant role, whereas the LUMO shows similarities to that of $[(btmgb)PtCl(dmso)]^+$. Additional coupled-cluster calculations using the CC2 method were carried out for btmgb and **5**. The structures were optimized and, subsequently, excitation energies and intensities were calculated. These CC2 calculations yielded results, but they were problematic because the values for the D_1 diagnostics[29] (0.14 for **5** and 0.08 for btmgb) clearly lie outside the range ($D_1(CC2) = 0.05$) over which the method can be expected to perform well. The spectra obtained are shown in the Supporting Information. (To display the spectra, the calculated transitions are folded by Gaussian functions with a standard deviation of $\sigma = 20$ nm.) The calculated spectra seem to reproduce the essentials of the observed spectra well. The experimental spectrum of btmgb shows no absorption between $\lambda = 600$ and 350 nm, and has a band with a maximum around 300 nm. Likewise, the calculated spectrum shows no absorption in the longer-wavelength region, but an intense absorption between $\lambda = 300$ and 200 nm. The experimental spectrum of **5** is characterized by additional absorptions at longer wavelengths, namely at $\lambda = 470$, 360, and

310 nm. Likewise the calculated spectrum features an absorption maximum at $\lambda = 430$ nm, and furthermore a shoulder at $\lambda = 320$ nm and a maximum at $\lambda = 270$ nm. Hence, the basic difference between observed and calculated spectra appears to be a shift by about 40 nm. The main contribution to the transition calculated at about 430 nm stems from the excitation of the 58a′ orbital (HOMO) to the 52a″ (LUMO+1) orbital (see the Supporting Information for isodensity plots). Both orbitals are delocalized over the Pt center, the guanidino unit, and the benzene ring, but within the 58a′ orbital the contribution from the guanidino unit is localized at the nitrogen bound to the Pt center, whereas within the 52a″ orbital it is localized at the central carbon atom of the guanidino unit. Hence, some charge transfer to the central carbon atom of the guanidino group can be assigned to the transition at $\lambda = 430$ nm.

[(hpp)(hppH)PtCl$_2${N(H)C(O)CH$_3$}] (6): In compounds **3**–**5** the guanidine acts as a neutral ligand. For guanidines such as hppH, which feature a hydrogen atom bound to the N atom, proton elimination occurs easily, leading to the hpp$^-$ anion, which could act as a η^1- or η^2-coordinating ligand as well as a bridging (μ^2) ligand. An example of a complex with bridging guanidinate ligands and Pt in a high oxidation state is [Pt$_2$(hpp)$_4$Cl$_2$] with its characteristic paddlewheel structure,[30] in which the Pt atoms are engaged in direct and multiple metal–metal bonding (and thus formally containing a Pt_2^{6+} dimer). From a simple consideration of orbital orientation it has been claimed that hpp$^-$ prefers μ coordination over η^2 coordination, a rule which indeed many compounds obey.[28,31] Recently we have reported on the bisguanidine complex [(hppH)$_2$PtCl$_2$], which can be synthesized in its *cis* as well as in its *trans* form.[22] In new experiments *cis*-[(hppH)$_2$PtCl$_2$], dissolved in CH$_3$CN, was treated with a 30% H_2O_2 aqueous solution. Oxidation of Pt^{II} to Pt^{IV} was followed by a color change from yellow to orange, giving an oily product, which we were not able to crystallize or characterize adequately. A small number of crystals were grown from an acetone/hexane mixture. The single-crystal analysis showed that these crystals consisted of [(η^2-hpp)(hppH)PtCl$_2${N(H)C(O)CH$_3$}] molecules, **6** (see Figure 6), which are formed by the pathway shown in Scheme 3. H_2O_2 reacts first with *cis*-[(hppH)$_2$PtCl$_2$] to give [(η^2-hpp)(hppH)PtCl$_2$(OH)], which is likely to be the oily compound. The acetamido species **6** is formed by conversion of solvent (CH$_3$CN) molecules in the ligand sphere. Such a process has been reported in the literature for other Pt complexes.[32] The most interesting structural feature of **6** (see Table 7) is the bonding mode of the hpp$^-$ ligand. The N4···N5 separation (220.1(2) pm) is short, and the angle N4-C8-N5 is only 108.6(3)°. For comparison, the N1···N2 bond length and N1-C1-N2 bond angle within the η^1-coordinated hppH ligand are 232.1(3) pm and 120.0(4)°. The Pt atom is coordinated in a distorted octahedral fashion by three N, two Cl, and one O atom. The N4-Pt-N5 angle (64.2(1)°) is much smaller and the N4-Pt-Cl1 angle much larger (103.0(1)°) than the 90° angle of an octahedron.

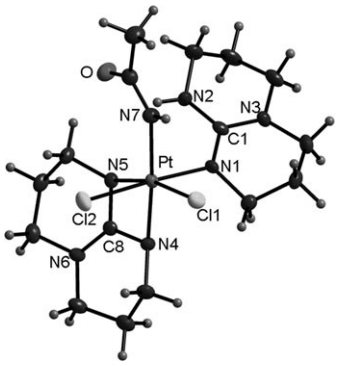

Figure 6. Crystal structure of **6**. Ellipsoids are drawn at the 50% probability level.

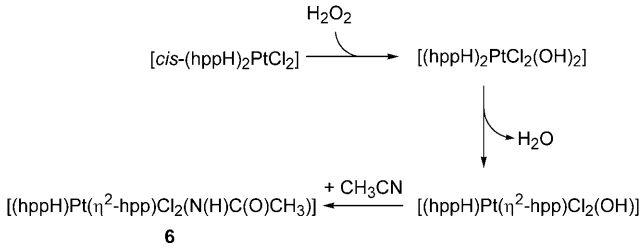

Scheme 3. Synthesis of complex **6**.

Table 7. Selected bond lengths [pm] and angles [°] of **6** as obtained by X-ray diffraction studies(see Figure 6 for atom numbering).

Pt–Cl1	235.1(1)	Pt–Cl2	232.9(1)
Pt–N7	203.6(4)	Pt–N1	203.8(3)
Pt–N4	206.5(3)	Pt–N5	207.0(3)
Pt···C8	247.6(1)	Pt···HN2	281.9(3)
N2–C1	135.4(5)	N1–C1	132.4(5)
N3–C1	134.3(5)	N2–H	87(5)
N4–C8	134.7(5)	N5–C8	135.9(5)
N6–C8	132.4(5)		
Cl1-Pt-Cl2	89.6(4)	N4-Pt-N5	64.2(1)
N1-Pt-Cl1	90.3(1)	N1-Pt-Cl2	176.8(1)
N1-Pt-N4	88.0(1)	N1-Pt-N5	92.3(1)
N4-Pt-Cl1	103.0(1)	N4-Pt-Cl2	88.9(1)
N5-Pt-Cl1	166.8(1)	N7-Pt-N2	92.5(2)
N7-Pt-N4	173.8(1)	N7-Pt-N5	109.6(1)
N7-Pt-Cl1	83.2(1)	N7-Pt-Cl2	90.7(1)
N1-C1-N2	119.9(4)	N4-C8-N5	108.6(3)

To find out whether CH$_3$COOH elimination from **6** is possible leading to the Pt^{IV} complex [(η^2-hpp)$_2$PtCl$_2$], **7**, further quantum chemical calculations were carried out which indicate that **7** is indeed a stable species (see Figure 7 for an illustration of its likely structure and Table 8 for selected bond lengths and angles). An energy change $\Delta_R E$ of $+48$ kJ mol^{-1} is calculated to be associated with the (gas-phase) reaction set out in Equation (2); at $T = 298$ K $\Delta_R G^{\ominus} = -12$ kJ mol^{-1}.

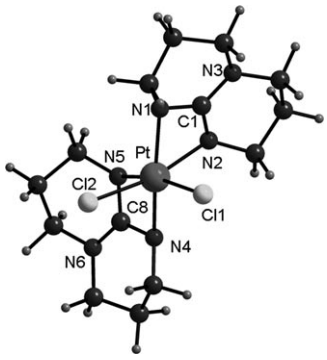

Figure 7. Calculated structure of **7**.

Table 8. Selected calculated bond lengths [pm] and angles [°] of **7** (see Figure 7 for atom numbering).

Pt–Cl1	237.7	Pt–Cl2	237.9
Pt–N1	208.8	Pt–N2	208.1
Pt–N4	208.3	Pt–N5	208.3
N1–C1	133.5	N2–C1	134.0
N4–C8	133.9	N5–C8	133.7
N3–C1	135.4	N6–C8	134.9
N1-Pt-N2	63.4	N4-Pt-N5	63.5
Cl1-Pt-Cl2	93.2	N1-Pt-N4	162.9
N1-Pt-N5	104.1	N1-Pt-Cl1	88.0
N1-Pt-Cl2	103.6	Cl2-Pt-N2	166.8
Cl1-Pt-N5	167.0	N4-Pt-Cl1	103.7
N4-Pt-Cl2	88.4	N4-Pt-N2	103.9

$$[(\eta^2\text{-hpp})(\text{hppH})\text{PtCl}_2(\text{OAc})] \rightarrow [(\eta^2\text{-hpp})_2\text{PtCl}_2] + \text{HOAc} \quad (2)$$

On the basis of these theoretical results it is plausible that **7** could be formed as well. Indeed, the NMR spectra of the reaction mixture (see the Supporting Information) indicate the presence of more than one reaction product.

Conclusion

Reaction of 1,2-bis(*N*,*N*,*N*′,*N*′-tetramethylguanidino)benzene (btmgb) with $H_2O{\cdot}B(C_6F_5)_3$ leads to protonation and formation of the salt $[\text{btmgbH}]^+[\text{HOB}(C_6F_5)_3]^-$. In the $[\text{btmgbH}]^+$ cation the proton is bound to only one N atom, in agreement with quantum chemical calculations. In contrast to proton sponges such as 1,8-bis(*N*,*N*,*N*′,*N*′-tetramethylguanidino)naphthalene (btmgn) there is no significant interaction with the second imine N atom. The $[\text{btmgbH}_2]^{2+}$ dication also was characterized structurally. The experiments showed that btmgb could be used as a chelating ligand. The new Pt complexes $[(\text{btmgb})\text{PtCl}_2]$, $[(\text{btmgb})\text{PtCl(dmso)}][\text{PtCl}_3(\text{dmso})]$ and [(btmgb)PtCl(dmso)]Cl were prepared and characterized. According to X-ray diffraction analysis results, upon coordination of Pt^{II} the imine N=C bond lengths of btmgb increase dramatically: in $[(\text{btmgb})\text{PtCl}_2]$ and $[(\text{btmgb})\text{PtCl(dmso)}][\text{PtCl}_3(\text{dmso})]$ they increase by about 6 pm. A new Pt^{IV} complex with a chelating guanidinate, $[(\eta^2\text{-hpp})(\text{hppH})\text{PtCl}_2\{\text{N(H)C(O)CH}_3\}]$, in which the hpp^- ligand is η^2-coordinated, was synthesized also.

Experimental Section

All synthetic work was carried out by using standard Schlenk techniques. IR spectra were recorded by using a BIORAD Excalibur FTS 3000 spectrometer. NMR spectra were measured by means of a Bruker Avance II 400 spectrometer. A Perkin–Elmer Lambda 19 spectrometer was used for recording UV/Vis spectra. The ligand btmgb was synthesized as described in the literature.[9]

$[\text{btmgbH}]^+[\text{HOB}(C_6F_5)_3]^-$ (1): The ligand btmgb (0.079 g. 0.26 mmol) and $H_2O{\cdot}B(C_6F_5)_3$ (0.133 g, 0.25 mmol) were stirred in toluene at room temperature for 1 h. After removal of the solvent the remaining white solid was crystallized from CH_3CN. White crystals of **1** (0.106 g, 0.13 mmol) were obtained. Yield 52%; ^{1}H NMR (399.89 MHz, CD_3CN): $\delta = 6.95$–6.92 (m, 2H), 6.71–6.68 (m, 2H), 2.78 ppm (s, 24H; CH_3); ^{13}C NMR (100.56 MHz, CD_3CN): $\delta = 160.87$, 137.51, 123.88, 122.07, 40.19 ppm (CH_3); ^{11}B NMR (128.30 MHz, CD_3CN): $\delta = -3.95$ ppm; ^{19}F NMR (376.23 MHz, CD_3CN): $\delta = -135.54$, -161.70, -165.66 ppm; IR (CsI): $\tilde{\nu} = 3690$ (w), 2939 (w), 1644 (m), 1616 (m), 1583 (s), 1562 (vs), 1515 (vs), 1464 (vs), 1425 (m), 1386 (m), 1276 (w), 1161 (w), 1082 (s), 959 (s), 810 (w), 770 (w), 748 (w), 673 cm^{-1} (w); MS (ESI,CH_3CN): *m*/*z* (%): 305 (100) $[\text{btmgbH}]^+$, 260 (8.5) $[\text{btmgbH}-\text{HN(CH}_3)_2]^+$.

$[\text{btmgbH}_2]\text{Cl}_2$ (2): The ligand btmgb (0.65 g, 2.14 mmol) was dissolved in HCl (5 mL, 1 M). Subsequently the water was removed and the remaining solid was crystallized from CH_3CN. The crystals were dried under vacuum to give **2** (0.584 g, 1.55 mmol) as a white solid. Yield 73%; ^{1}H NMR (199.92 MHz, CD_3CN): $\delta = 11.24$ (s, 2H), 7.31–7.22 (m, 2H), 7.01–6.92 (m, 2H), 2.97 ppm (s, 24H; CH_3); ^{13}C NMR (50.28 MHz, CD_3CN): $\delta = 159.64$, 131.16, 127.51, 123.96, 41.27 ppm (CH_3); IR (CsI): $\tilde{\nu} = 3433$ (s), 3344 (s), 2951 (m), 1639 (vs), 1602 (s), 1549 (vs), 1489 (m), 1478 (s), 1449 (m), 1406 (s), 1307 (s), 1231 (s), 1167 (m), 1068 (w), 1036 (m), 913 (w), 866 (w), 782 (m), 756 (m), 504 cm^{-1} (m); MS (EI): *m*/*z* (%): 305 (39) $[\text{btmgbH}]^+$, 260 (44) $[\text{btmgbH}-\text{HN(CH}_3)_2]^+$, 233 (37) $[\text{btmgbH}-\text{HN(CH}_3)_2-\text{HCN}]^+$, 188 (91) $[\text{btmgbH}-2\text{HN(CH}_3)_2-\text{HCN}]^+$ 108 (74) $[C_6H_8N_2]^+$.

$[(\text{btmgb})\text{PtCl(dmso)}]^+[\text{PtCl}_3(\text{dmso})]^-$ (3): A solution of *cis*-$[(\text{dmso})_2\text{PtCl}_2]$ (0.236 g, 0.559 mmol) in CH_3CN (15 mL) containing and btmgb (0.176 g, 0.578 mmol) was stirred for 1 h at room temperature. The solvent was removed under vacuum and the remaining oil was dissolved again in acetone ($\approx$7 mL). From this solution **3** (0.146 g, 0.147 mmol) was precipitated as orange crystals. Yield 53%; ^{1}H NMR (399.89 MHz, CD_3CN): $\delta = 6.72$–6.68 (m, 2H), 6.37–6.31 (m, 2H), 3.36 (s, 6H; dmso), 3.26 (s, 6H; dmso), 3.10 (s, 6H; CH_3), 3.08 (s, 6H; CH_3), 3.02 (s, 6H; CH_3), 2.99 ppm (s, 6H; CH_3); ^{13}C NMR (100.56 MHz, CD_3CN): $\delta =$ 166.88, 165.38, 143.82, 143.74, 121.79, 121.77, 115.73, 114.64, 45.53 (dmso), 43.92 (dmso), 41.68 (CH_3), 41.52 (CH_3), 40.97(CH_3), 40.28 ppm (CH_3); ^{195}Pt NMR (85.96 MHz, CD_3CN): $\delta = -2962.34$, -2979.24 ppm; IR (CsI): $\tilde{\nu} = 3003$ (w), 2918 (w), 1606 (s), 1592 (vs), 1580 (s), 1515 (vs), 1488 (vs), 1443 (m), 1400 (vs), 1316 (s), 1277 (s), 1225 (m), 1163 (m), 1136 (s), 1030 (s), 921 (w), 876 (w), 845 (w), 735 (m), 694 (w), 443 cm^{-1} (w); UV/Vis ($CHCl_3$, $c = 4.8\times10^{-5}$ mol L^{-1}): $\lambda_{max}(\varepsilon) = 431$ (2240), 341 (4926), 292 nm (14479 dm^3 mol^{-1} cm^{-1}); MS (FAB): *m*/*z* (%): 613 (100) $[(\text{btmgb})\text{Pt(dmso)Cl}]^+$, 570 (9) $[(\text{btmgb})\text{Pt(Cl)}_2]^+$, 534 (26) $[(\text{btmgb})\text{PtCl}]^+$, 499 (69) $[(\text{btmgb})\text{Pt}]^{2+}$, 454 (15) $[(\text{btmgb})\text{Pt}-\text{N(CH}_3)_2]^{2+}$, 409 (17) $[(\text{btmgb})\text{Pt}-2\text{N(CH}_3)_2]^{2+}$.

$[(\text{btmgb})\text{PtCl(dmso)}]^+\text{Cl}^-$ (4): *cis*-$[(\text{dmso})_2\text{PtCl}_2]$ (0.253 g, 0.599 mmol) was dissolved in DMSO (15 mL), btmgb (0.192 g, 0.631 mmol) was added, and the reaction mixture was stirred for 1 h at room temperature. Half of the DMSO was removed and acetone (5 mL) was added. A yellow solid (**4**) (0.295 g, 0.454 mmol) was precipitated. Yield 76%; ^{1}H NMR (399.89 MHz, CD_3CN): $\delta = 6.72$–6.67 (m, 2H), 6.36–6.31 (m, 2H), 3.36 (s, 6H; dmso), 3.09 (s, 6H; CH_3), 3.08 (s, 6H; CH_3), 3.02 (s, 6H; CH_3), 2.99 ppm (s, 6H; CH_3); ^{13}C NMR (100.56 MHz, CD_3CN): $\delta =$

166.90, 165.40, 143.82, 143.75, 121,78, 121.77, 115.74, 114.64, 45.50 (dmso), 41.66 (CH_3), 41.51 (CH_3), 40.95(CH_3), 40.27 ppm (CH_3); ^{195}Pt NMR (85.96 MHz, CD_3CN): $\delta = -2979.49$; IR (CsI): $\tilde{\nu} = 3013$ (w), 2928 (w), 1599 (vs), 1578 (s), 1520 (vs), 1485 (s), 1470 (s), 1416 (s), 1395 (vs), 1323 (s), 1275 (m), 1225 (m), 1167 (m), 1141 (s), 1035 (m), 1009 (w), 920 (w), 871 (w), 841 (w), 752 (m), 441 cm^{-1} (w); UV/Vis ($CHCl_3$, $c = 5{,}9 \times 10^{-5}$ mol L^{-1}): λ_{max} (ε) = 432 (2159), 341 (4564), 292 nm (13828 $dm^3 mol^{-1} cm^{-1}$); MS (ESI,CH_2Cl_2): *m*/*z* (%): 612 (100) [*M*−l]; MS (FAB): *m*/*z* (%): 613 (90) [(btmgb)Pt(dmso)Cl]$^+$, 534 (26) [(btmgb)PtCl]$^+$, 499 (78) [(btmgb)Pt]$^{2+}$, 454 (9) [(btmgb)Pt−N$(CH_3)_2$]$^{2+}$, 409 (12) [(btmgb)Pt−2N$(CH_3)_2$]$^{2+}$.

[(btmgb)PtCl$_2$] (5): Compound **4** (0.188 g, 0.290 mmol) was heated for 4 h under vacuum to 150 °C. A red compound was formed. Upon recrystallization from toluene/dichloromethane (6:1, v/v) red crystals of **5** (0.155 g, 0.272 mmol) were obtained. Yield 94 %; ^{1}H NMR (399.89 MHz, CD_3CN): $\delta = 6.61$–6.57 (m, 2H), 6.24–6.20 (m, 2H), 3.01 (s, 12H; CH_3), 2.96 ppm (s, 12H; CH_3); ^{13}C NMR (100.56 MHz, CD_3CN): $\delta = 167.76$, 146.13, 121.06, 116.23, 41.23 (CH_3), 39.80 ppm (CH_3); ^{195}Pt NMR (85.96 MHz, CD_3CN): $\delta = -1848.60$ ppm; IR (CsI): $\tilde{\nu} = 2936$ (w), 1594 (s), 1576 (vs), 1514 (vs), 1489 (s), 1400 (vs), 1323 (m), 1281 (m), 1217 (m), 1167 (m), 1036 (m), 920 (w), 871 (w), 839 (w), 756 (m), 697 cm^{-1} (w); UV/Vis ($CHCl_3$, $c = 6{,}7 \times 10^{-5}$ mol L^{-1}): λ_{max} (ε) = 469 (4087), 361 (12141), 313 nm (21268 $dm^3 mol^{-1} cm^{-1}$); MS (FAB): *m*/*z* (%): 571 (60) [(btmgb)PtCl$_2$]$^+$, 534 (19) [(btmgb)PtCl]$^+$, 498 (24) [(btmgb)Pt]$^{2+}$, 454 (9) [(btmgb)Pt−N$(CH_3)_2$]$^{2+}$, 409 (12) [(btmgb)Pt−2N$(CH_3)_2$]$^{2+}$.

[(hpp)(hppH)PtCl$_2${N(H)C(O)CH$_3$}] (6): *cis*-[$(hppH)_2PtCl_2$] (144 mg), prepared from reaction of [$hppH_2$]$_2$[$PtCl_4$] with Li(hpp) and also containing some $hppH_2Cl$ and [$(hppH)_3PtCl$]Cl (which are very difficult to eliminate), was dissolved in CH_3CN (10 mL). Slow addition of H_2O_2 solution (0.6 mL in total, 30 %) resulted in the solution changing color from yellow to orange. It was stirred for 20 h at room temperature, then the solvent was removed under vacuum. The orange residue was washed several times with diethyl ether, dissolved in acetone, and filtered from silica. After removal of the solvent an orange oil remained. Crystals were obtained from a solution of acetone layered with hexane at 0 °C. The ^{1}H NMR spectra showed the presence of molecules of more than one product (see Discussion and the Supporting Information) so that unambiguous identification of the signals due to **6** proved impossible.

X-ray crystallography: Suitable crystals were taken directly out of the mother liquor, immersed in perfluorinated polyether oil, and fixed on top of a glass capillary. Measurements were made on a Nonius-Kappa CCD diffractometer with a low-temperature unit using graphite-monochromated MoK_α radiation. The temperature was set to 200 K. The data collected were processed using the standard Nonius software.[33] All calculations were performed using the SHELXT-PLUS software package. Structures were solved by direct methods with the SHELXS-97 program and refined with the SHELXL-97 program.[34,35] Graphical handling of the structural data during solution and refinement was performed with XPMA.[36] Atomic coordinates and anisotropic thermal parameters of non-hydrogen atoms were refined by full-matrix least-squares calculations.

CCDC-676968 (**1**), 676969 (**2**), 676966 (**3**), 676967 (**5**), 676970 (**6**) and 677131 (free btmgb ligand) contain the supplementary crystallographic data (excluding structure factors) for this paper. These data can be obtained free of charge from The Cambridge Crystallographic Data Centre via www.ccdc.cam.ac.uk/data_request/cif.

Quantum chemical calculations: The quantum chemical calculations within the framework of density functional theory were performed with the TURBOMOLE program package.[37] In all calculations the B3LYP functional[38] was employed and the def2-TZVP basis set[39] was used for all atoms. This required the use of an effective core potential on Pt[40] representing 60 core electrons. The structures were optimized.

In addition, coupled cluster calculations using the CC2 method[41] were performed for btmgb and complex **5**. The structures were optimized and subsequently excitation energies and intensities were calculated. The calculations used the def2-SVP basis set[39] on Pt and the def2-SV(P) basis set[39] on all other atoms. Within the calculations, the resolution-of-the-identity approximation was employed to calculate the two-electron integrals. Therefore, the appropriate def2-SV(P) and def2-SVP auxiliary basis sets[42] were used. The calculations were performed with the TURBOMOLE program system.[37] The underlying HF calculations used the DSCF module;[43] the CC2 calculations used the RI-CC2 module.[44]

Acknowledgements

Financial support by the Deutsche Forschungsgemeinschaft (DFG), especially through the priority program 1178, and the Fonds der Chemischen Industrie is gratefully acknowledged.

[1] V. Raab, J. Kipke, R. M. Gschwind, J. Sundermeyer, *Chem. Eur. J.* **2002**, *8*, 1682–1693.
[2] a) J. A. Schellmann, *Biophys. Chem.* **2002**, *96*, 91–101; b) C. Tanford, *Adv. Protein Chem.* **1970**, *24*, 1–95.
[3] See, for example: E. P. O'Brien, R. I. Dima, B. Brooks, D. Thirumalai, *J. Am. Chem. Soc.* **2007**, *129*, 7346–7353.
[4] See, for example: a) M. Haj-Zaroubi, N. W. Mitzel, F. P. Schmidtchen, *Angew. Chem.* **2002**, *114*, 111–114; *Angew. Chem. Int. Ed.* **2002**, *41*, 104–107; b) S. L. Wiskur, J. J. Lavigne, A. Metzger, S. L. Tobey, V. Lynch, E. V. Anslyn, *Chem. Eur. J.* **2004**, *10*, 3792–3804.
[5] F. Otón, A. Espinosa, A. Tárraga, C. Ramírez de Arellano, P. Molina, *Chem. Eur. J.* **2007**, *13*, 5742–5753.
[6] S. Herres-Pawlis, A. Neuba, O. Seewald, T. Seshadri, H. Egold, U. Flörke, G. Henkel, *Eur. J. Org. Chem.* **2005**, 4879–4890.
[7] H. Wittmann, A. Schorm, J. Sundermeyer, *Z. Anorg. Allg. Chem.* **2000**, *626*, 1583–1590.
[8] S. Pohl, M. Harmjanz, J. Schneider, W. Saak, G. Henkel, *J. Chem. Soc. Dalton Trans.* **2000**, 3473–3479.
[9] M. Kawahata, K. Yamaguchi, T. Ito, T. Ishikawa, *Acta Crystallogr., Sect. E: Struct. Rep. Online* **2006**, *62*, o3301–o3302.
[10] P. Pruszynski, K. T. Leffek, B. Borecka, T. S. Cameron, *Acta Crystallogr. Sect. C: Cryst. Struct. Commun.* **1992**, *48*, 1638–1641.
[11] V. Raab, J. Kipke, O. Burghaus, J. Sundermeyer, *Inorg. Chem.* **2001**, *40*, 6964–6971.
[12] C. Würtele, E. Gaoutchenova, K. Harms, M. C. Holthausen, J. Sundermeyer, S. Schindler, *Angew. Chem.* **2006**, *118*, 3951–3954; *Angew. Chem. Int. Ed.* **2006**, *45*, 3867–3869.
[13] D. Maiti, D.-H. Lee, K. Gaoutchenova, C. Würtele, M. C. Holthausen, A. A. N. Sarjeant, J. Sundermeyer, S. Schindler, K. D. Karlin, *Angew. Chem.* **2007**, *120*, 88–91; *Angew. Chem. Int. Ed.* **2006**, *45*, 82-85.
[14] S. Li, H. Xie, S. Zhang, Y. Liu, J. Xu, J. Cao, *Synlett* **2005**, 1885–1888.
[15] A. Di Saverio, F. Focante, I. Camurati, L. Resconi, T. Beringhelli, G. D'Alfonsoi, D. Donghi, D. Maggioni, P. Mercandelli, A. Sironi, *Inorg. Chem.* **2005**, *44*, 5030–5041.
[16] a) G. C. Welch, R. R. S. Juan, J. D. Masuda, D. W. Stephan, *Science* **2006**, *314*, 1124–1126; b) P. A. Chase, G. C. Welch, T. Jurca, D. W. Stephan, *Angew. Chem.* **2007**, *119*, 9296; *Angew. Chem. Int. Ed.* **2007**, *46*, 9136.
[17] F. Focante, I. Camurati, L. Resconi, S. Guidotti, T. Beringhelli, G. D'Alfonso, D. Donghi, D. Maggioni, P. Mercandelli, A. Sironi, *Inorg. Chem.* **2006**, *45*, 1683–1692.
[18] B. Kovaćević, Z. B. Maksić, R. Vianello, M. Primorac, *New J. Chem.* **2002**, *26*, 1329–1334.
[19] Z. B. Maksić, B. Kovaćević, *J. Chem. Soc. Perkin Trans. 2* **1999**, 2623–2629.
[20] In contrast to the earlier calculation, our calculations found two additional minima for the [btmgbH]$^+$ cation (see the Supporting Information). In one of these minima the proton is engaged in intramolecular hydrogen bonding to the second imine N atom. It might be possible to verify this structure experimentally by using very weakly coordinating anions.
[21] R. S. Osborn, D. Rogers, *J. Chem. Soc. Dalton Trans.* **1974**, 1002–1004.

[22] H.-U. Wüstefeld, W. C. Kaska, F. Schüth, G. D. Stucky, X. Bu, B. Krebs, *Angew. Chem.* **2001**, *113*, 3280–3282; *Angew. Chem. Int. Ed.* **2001**, *40*, 3182–3184.
[23] U. Wild, P. Roquette, E. Kaifer, J. Mautz, H. Wadepohl, H.-J. Himmel, *Eur. J. Inorg. Chem.* **2008**, 1248-1257.
[24] R. Romeo, D. Minniti, S. Lanza, M. LL. Tobe, *Inorg. Chim. Acta* **1977**, *22*, 87–91.
[25] F. P. Fanizzi, L. Maresca, G. Natile, M. Lanfranchi, A. M. Manotti-Lanfredi, A. Tiripicchio, *Inorg. Chem.* **1988**, *27*, 2422–2431.
[26] F. P. Fanizzi, F. P. Intini, L. Maresca, G. Natile, G. Uccellobarretta, *Inorg. Chem.* **1990**, *29*, 29–33.
[27] H. C. Fry, C. Deal, E. Barr, S. D. Cummings, *J. Photochem. Photobiol. A* **2002**, *150*, 37–40.
[28] G. Annibale, M. Bonivento, L. Canovese, L. Cattalini, G. Michelon, M. L. Tobe, *Inorg. Chem.* **1985**, *24*, 797–800.
[29] C. L. Janssen, I. M. B. Nielsen, *Chem. Phys. Lett.* **1998**, *290*, 423.
[30] a) R. Clérac, F. A. Cotton, L. M. Daniels, J. P. Donahue, C. A. Murillo, D. J. Timmons, *Inorg. Chem.* **2000**, *39*, 2581–2584; b) F. A. Cotton, C. A. Murillo, X. Wang, C. C. Wilkinson, *Inorg. Chim. Acta* **2003**, *351*, 191–200.
[31] For work by our group, see: a) G. Robinson, C. Y. Tang, R. Köppe, A. R. Cowley, H.-J. Himmel, *Chem. Eur. J.* **2007**, *13*, 2648–2654; b) O. Ciobanu, P. Roquette, S. Leingang, H. Wadepohl, J. Mautz, H.-J. Himmel, *Eur. J. Inorg. Chem.* **2007**, 4530–4534; c) R. Dinda, O. Ciobanu, H. Wadepohl, O. Hübner, R. Acharraya, H.-J. Himmel, *Angew. Chem.* **2007**, *119*, 9270–9273; *Angew. Chem. Int. Ed.* **2007**, *46*, 9110–9113.
[32] C. M. Jensen, W. C. Trogler, *J. Am. Chem. Soc.* **1986**, *108*, 723–729.
[33] DENZO-SMN, Data processing software, Nonius **1998**; http://www.nonius.com.
[34] a) G. M. Sheldrick, *SHELXS-97*, *Program for Crystal Structure Solution*, University of Göttingen, **1997**; http://shelx.uni-ac.gwdg.de/SHELX/index.html; b) G. M. Sheldrick, *SHELXL-97*, *Program for Crystal Structure Refinement*, University of Göttingen, **1997**; http://shelx.uni-ac.gwdg.de/SHELX/index.html.
[35] *International Tables for X-ray Crystallography, Vol. 4*, Kynoch Press, Birmingham, U.K., **1974**.
[36] L. Zsolnai, G. Huttner, *XPMA*, University of Heidelberg, **1994**; http://www.uni-heidelberg.de/institute/fak12/AC/huttner/software/software.html.
[37] a) R. Ahlrichs, M. Bär, M. Häser, H. Horn, C. Kölmel, *Chem. Phys. Lett.* **1989**, *162*, 165–169; b) O. Treutler, R. Ahlrichs, *J. Chem. Phys.* **1995**, *102*, 346–356.
[38] P. J. Stephens, F. J. Dertin, C. F. Chabalonoski, M. J. Frisch, *J. Phys. Chem.* **1994**, *98*, 11623–11627.
[39] F. Weigend, R. Ahlrichs, *Phys. Chem. Chem. Phys.* **2005**, *7*, 3297–3305.
[40] D. Andrae, U. Häussermann, M. Dolg, H. Stoll, H. Preuss, *Theor. Chim. Acta* **1990**, 123–141.
[41] O. Christiansen, H. Koch, P. Jørgensen, *Chem. Phys. Lett.* **1995**, *243*, 409–418.
[42] F. Weigend, M. Häser, H. Patzelt, R. Ahlrichs, *Chem. Phys. Lett.* **1998**, *294*, 143–152.
[43] M. Häser, R. Ahlrichs, *J. Comput. Chem.* **1989**, *10*, 104–111.
[44] a) C. Hättig, F. Weigend, *J. Chem. Phys.* **2000**, *113*, 5154–5161; b) C. Hättig, A. Köhn, *J. Chem. Phys.* **2002**, *117*, 6939–6951; c) C. Hättig, *J. Chem. Phys.* **2003**, *118*, 7751–7761.
[45] Z. B. Maksić; personal communication.

Received: February 7, 2008
Published online: July 21, 2008

